Supporting Information for:

Synergistic Valorization of Spent Lithium-Ion Battery Electrodes: Anode Graphite Derived Lamellar Graphene Oxide Membranes for Selective Lithium Recovery from Cathode Leachate

Ying Zheng[a,b§], Ziwen Dai[a,c§], Zhaoyang Li[a,c], Guang Hu[a,c], Sha Liang[a,c], Wenbo Yu[a,c], Shushan Yuan[a,c**], Huabo Duan[a,c], Liang Huang[a,c], Jingping Hu[a,c], Huijie Hou [a,c], Jiakuan Yang[a,c,d*]

[a] Hubei Key Laboratory of Multi-media Pollution Cooperative Control in Yangtze Basin, School of Environmental Science & Engineering, Huazhong University of Science and Technology (HUST), 1037 Luoyu Road, Wuhan, Hubei, 430074, China

[b] School of Urban Construction, Wuchang Shouyi University, 22 Nanli Road, Wuhan, Hubei 430064, China

[c] Hubei Provincial Engineering Laboratory of Solid Waste Treatment, Disposal and Recycling, Huazhong University of Science and Technology (HUST), 1037 Luoyu Road, Wuhan, Hubei 430074, China

[d] State Key Laboratory of Coal Combustion, Huazhong University of Science and Technology (HUST), 1037 Luoyu Road, Wuhan, Hubei 430074, China

*Corresponding Author:

Prof. Jiakuan Yang, E-mail: jkyang@hust.edu.cn, Tel.: +86-27-87540995.

Prof. Shushan Yuan E-mail:yuanss@hust.edu.cn, Tel.: +86-27-87792207.

Contents of Supporting Information

Text S1. Pretreatment of the spent graphite in the spent lithium-ion batteries (LIBs).....5

Text S2. Membrane separation experiments. 6

Table S1. Evolution of C-C bond length and lattice parameter during graphene oxide (GO) synthesis.....8

Table S2. Evolution of raman spectra during graphene oxide (GO) synthesis. 9

Table S3. Performance comparison of Li^+ flux *versus* Li^+/M^{2+} selectivity for the representative membranes.....10

Table S4 Economic analysis of recycling of 1 kg spent graphite in the spent lithium-ion batteries (LIBs). 12

Figure S1. Images of the graphene oxide (GO) membrane (deposition amount: 0.15g·m^{-2}). 14

Figure S2. C 1s spectrum of (a) spent graphite, (c) graphite oxide, and (e) graphene oxide (GO) ; O 1s spectrum of (b) spent graphite, (d) graphite oxide, and (f) graphene oxide (GO).. 15

Figure S3. (a, b) AFM 3D image; (c, d) AFM surface image of graphene oxide (GO) nanosheet; (e, f) Size of graphene oxide (GO) nanosheet.. 16

Figure S4. SEM images of the polyethersulfone (PES).....17

Figure S5. SEM images of the graphene oxide (GO) membrane (a, b, and c) and graphene oxide-polyethyleneimine (GO-PEI) membrane (d, e, and f) surface with the different graphene oxide (GO) deposition amounts: (a, d) 0.15g·m^{-2}; (b, e) 0.3 g·m^{-2}; (c, f) 0.6 g·m^{-2}. 18

Figure S6. EDS of the graphene oxide (GO) membrane (a, b, and c) and graphene oxide-polyethyleneimine (GO-PEI) membrane (d, e, and f) surface with the different graphene oxide (GO) deposition amounts: (a, d) 0.15g·m^{-2}; (b, e) 0.3 g·m^{-2}; (c, f) 0.6 g·m^{-2}. 19

Figure S7. (a) AFM surface image, and (b) surface roughness of graphene oxide (GO) (0.6) membrane. 20

Figure S8. The contact angles for graphene oxide (GO) membranes and graphene oxide-polyethyleneimine (GO-PEI) membranes with the different loadings: 0.15, 0.3, and 0.6 g·m^{-2}. 21

Figure S9. The potentials of (a) graphene oxide (GO) membrane, (b) GO (0.15)-polyethyleneimine (PEI) membrane, (c) GO (0.3)-PEI membrane, and (d) GO (0.6)-PEI membrane.....22

Figure S10. Activation energy for ion permeation through the GO(0.6)-PEI membrane. 23

Figure S11. (a) XRD pattern, and (b) SEM image of the recovered Li_2CO_3 product. 24

References.....25

Text S1. Pretreatment of the spent graphite in the spent lithium-ion batteries (LIBs).

The collected spent lithium-ion batteries (LIBs) were immersed in a 5% NaCl solution for thorough discharge. After discharging, the batteries were disassembled to obtain the anode sheets. These anode sheets were cut into small segments using scissors. The segments were then immersed in N-methylpyrrolidone (NMP) solution at 50 °C for 1 h to separate the graphite from the copper foil current collector. The separated graphite was subsequently oven-dried and ground. The ground material was sieved through a 300-mesh sieve. The powders were placed in an alumina crucible and calcined in a tube furnace at 500 °C for 2 h to remove residual binder and carbon black, yielding the final experimental material: the spent graphite.

Text S2. Membrane separation experiments.

The separation experiments primarily investigated the separation performance of Li^+ *versus* other divalent ions in leachates from single salts, mixed salts, and spent LIB cathode materials. All separation experiments were conducted in a bilateral diffusion cell with an effective membrane diameter of 8 mm. First, the membrane was installed in the diffusion cell. The diffusion cell was wetted with a 50% (wt.) ethanol/water mixture on both sides for 5 min. The cell was then rinsed three times with deionized (DI) water. Subsequently, DI water was added to the permeate side facing the base membrane, while the selective side was filled with either a single-salt solution (LiCl, $MgCl_2$, $CoCl_2$, $NiCl_2$, or $MnCl_2$) or a binary-salt mixture (LiCl/$MgCl_2$, LiCl/$CoCl_2$, LiCl/$NiCl_2$, or LiCl/$MnCl_2$) at a concentration of 0.1 mol L^{-1} or spent LIBs cathode leachate at a Li^+ concentration of 0.1 mol L^{-1}, Ni^{2+}, Co^{2+}, and Mn^{2+} concentration of 0.001 mol L^{-1}. Separation was carried out at a constant trans-membrane pressure of 1 atm and a temperature of 25 °C for 1 h. The solutions on both sides were stirred at 1500 rpm. Upon completion of each run, the salt concentrations in the permeate sides were determined by inductively coupled plasma optical emission spectroscopy (ICP-OES). The permeation flux J_s of individual ions was calculated by the following Equation S1.

$$J_S = \frac{CV \times 10^{-3}}{A \cdot t \cdot M} \quad \text{(S1)}$$

Where, J_S is the permeation flux of the single-salt ion ($mol \cdot m^{-2} \cdot h^{-1}$); C is the salt concentration on the permeate side after t hours of separation ($mg \cdot L^{-1}$); V is the volume of the salt solution on the permeate side after t hours of separation (L); A is the effective

membrane area (m^2); M is the molar mass of the salt ($g \cdot mol^{-1}$).

In the mixed-salt and spent LIBs cathode leachate separation experiments, the permeation flux of each ion was first calculated using the Equation S1 above, and the selectivity was subsequently determined according to Equation S2:

$$S = \frac{J_{S_1}}{J_{S_2}} \tag{S2}$$

where S is the monovalent-to-divalent ion selectivity; J_{S1} is the permeation flux of the monovalent ion ($mol \cdot m^{-2} \cdot h^{-1}$); J_{S2} is the permeation flux of the divalent ion ($mol \cdot m^{-2} \cdot h^{-1}$).

Furthermore, steady-state transmembrane permeation experiments were performed at 303 K, 313 K, 323 K and 333 K. Flux variations with temperature were recorded, and the activation energies (E_a) for the transmembrane transport of various ions were determined by linear fitting with a modified Arrhenius equation (Equation S3).

$$\ln F = \ln A - \frac{E_a}{RT} \tag{S3}$$

where F is the ion permeation flux ($mol \cdot m^{-2} \cdot h^{-1}$); E_a is the activation energy for transmembrane ion permeation ($kJ \cdot mol^{-1}$); R is the universal gas constant (8.314 $J \cdot mol^{-1} \cdot K^{-1}$); T is the absolute temperature (K); Ais the pre-exponential factor (a constant related to membrane structure and ionic characteristics).

Table S1. Evolution of C-C bond length and lattice parameter during graphene oxide (GO) synthesis.

Samples	Experimental d110 (Å)	d100 (Å)			C-C bond length l (Å)	Lattice parameter a (Å)
		Calculated Value	Experimental Value	Deviation Value		
Spent graphite	1.2323	2.1344	2.1400	0.0056	1.4229	2.4646
Graphite oxide	1.2410	2.1495	2.1175	-0.0320	1.4330	2.4820
GO	1.2354	2.1398	2.1160	-0.0238	1.4265	2.4708

The (100) d-spacing, C-C bond length, and lattice parameter were calculated by Equations S4-S6, respectively.

$$d_{100} = \sqrt{3} \times d_{110} = \frac{\sqrt{3}}{2} a \tag{S4}$$

$$a = 2 \times d_{110} \tag{S5}$$

$$l = \frac{a}{\sqrt{3}} \tag{S6}$$

Where, d_{100} is the d-spacing of (100) (Å); d_{110} is the d-spacing of (110) (Å); l is the length of C-C bond (Å); a is the lattice parameter (Å).

Table S2. Evolution of raman spectra during graphene oxide (GO) synthesis.

Samples	D Band /cm^{-1}		G Band /cm^{-1}		Intensity ratio	Average Crystallite Size
	Raman shift	FWHM	Raman shift	FWHM	(I_D/I_G)	L_a (nm)
Spent graphite	1402.4	327.4	1576.6	31.7	0.28	68.6
Graphite oxide	1360.2	200.9	1588.0	97.9	1.93	10.0
Graphene oxide (GO)	1355.8	203.9	1582.8	105.7	2.00	9.6

The average crystallite size was calculated by Equation S7.

$$L_a = (2.4\times10^{-10})\lambda^4 \cdot (I_D / I_G)^{-1} \quad \text{(S7)}$$

Where, L_a is the average crystallite size (nm); I_D/I_G is the ratio of intensity; λ is laser wavelength, 532 nm.

Table S3. Performance comparison of Li^+ flux *versus* Li^+/M^{2+} selectivity for the representative membranes.

Membrane	Li^+ permeation rate ($mol \cdot m^{-2} \cdot h^{-1}$)	Li^+/M^{2+} Selectivity	References
GO(0.6)-PEI	0.06977	52,856 (Li^+/Mn^{2+})	This work
TpBDMe2 COF	0.0383	35.8	Sheng et al., 2021
COF-4EO-PAN	0.034	64	Bing et al., 2025
M-2 membrane	0.015	13	Wu et al., 2023
PET~0.6 nm pore	0.01	~100	Wen et al., 2016
GO	0.32	1.45	Liang et al., 2020
Nafion	0.0115	2.07	Zhou et al., 2021
MXene	0.00105	3.33	Foller et al., 2021
MXene	0.014	2.6	Kang et al., 2023
Porous graphene	0.0511	25.08	
Porous graphene	0.0961	12.99	
Porous graphene	0.0231	55.79	Zhou et al., 2024
CMP-masked graphene	0.0103	232.3	
PA-g-TETA	0.00132	103.5	Li et al., 2023

PA-B2-E3	0.0677	12.7	Li et al., 2017
MXene/CNT	0.0491	54.5	Lu et al., 2019
COF	0.0553	217	Sheng et al., 2021
DMBP-TB	0.06	14.6	Tan et al., 2020

Table S4 Economic analysis of recycling of 1 kg spent graphite in the spent lithium-ion batteries (LIBs).

	Item	Unit price	Quantity	Cost ($)
Input	Spent graphite	0.46 $/kg [a]	1.00 kg	0.46
	Concentrated sulfuric acid	0.0065 $/ml [b]	60000 ml	834.79
	Concentrated phosphoric acid	0.022 $/ml [b]	5000 ml	
	Potassium permanganate	0.032 $/g [b]	10000 g	
	Hydrogen peroxide	0.0079 $/ml [b]	3000 ml	
	Industrial electricity	0.139 $/kw·h [c]	221.37 kW·h	30.77
	Industrial water	0.579 $/$m^3$ [d]	4.2 m^3	2.43
	Maintenance and Depreciation fees	0.53 $/kg [e]		0.53
	Personnel wages	0.30 $/kg [f]		0.30
	Hazardous waste disposal			424[g]
Output	Single-layer GO	2.1 $/g [h]	1000 g	2100
	Profit			806.72

a: The recycling cost for 1 kg of lithium cobalt oxide (LCO) batteries is approximately \$2,275.52 t^{-1}. Given that waste graphite accounts for 20% of the mass, the cost attributable to it is \$0.46 kg^{-1}.

b: The market price of concentrated sulfuric acid, concentrated phosphoric acid, potassium permanganate and hydrogen peroxide were provided by Sino pharm Chemical Reagent Co., Ltd. (https://www.reagent.com.cn/).

c: The industrial electricity price in Wuhan, China is $0.139 /kW·h.

d: The industrial water price in Wuhan, China is $0.579 /$m^3$.

e: The annual equipment maintenance and depreciation fees was calculated according to 3% of the cost of the equipment. The price of equipment ($6384.888) was obtained from https://prices.sci99.com. The input cost of equipment was $6384.888×3%÷365≈$0.53.

f: The labor wage of processing 1t spent lithium ion battery in the literature was $299.589.

g: According to the actual situation of hazardous waste disposal in Hubei Province, China, the disposal cost of the wastes generated per 1 kilogram of GO produced was $424.

h: The values of GO was obtained from https://prices.sci99.com.

Figure S1. Images of the graphene oxide (GO) membrane (deposition amount: 0.15g·m^{-2})

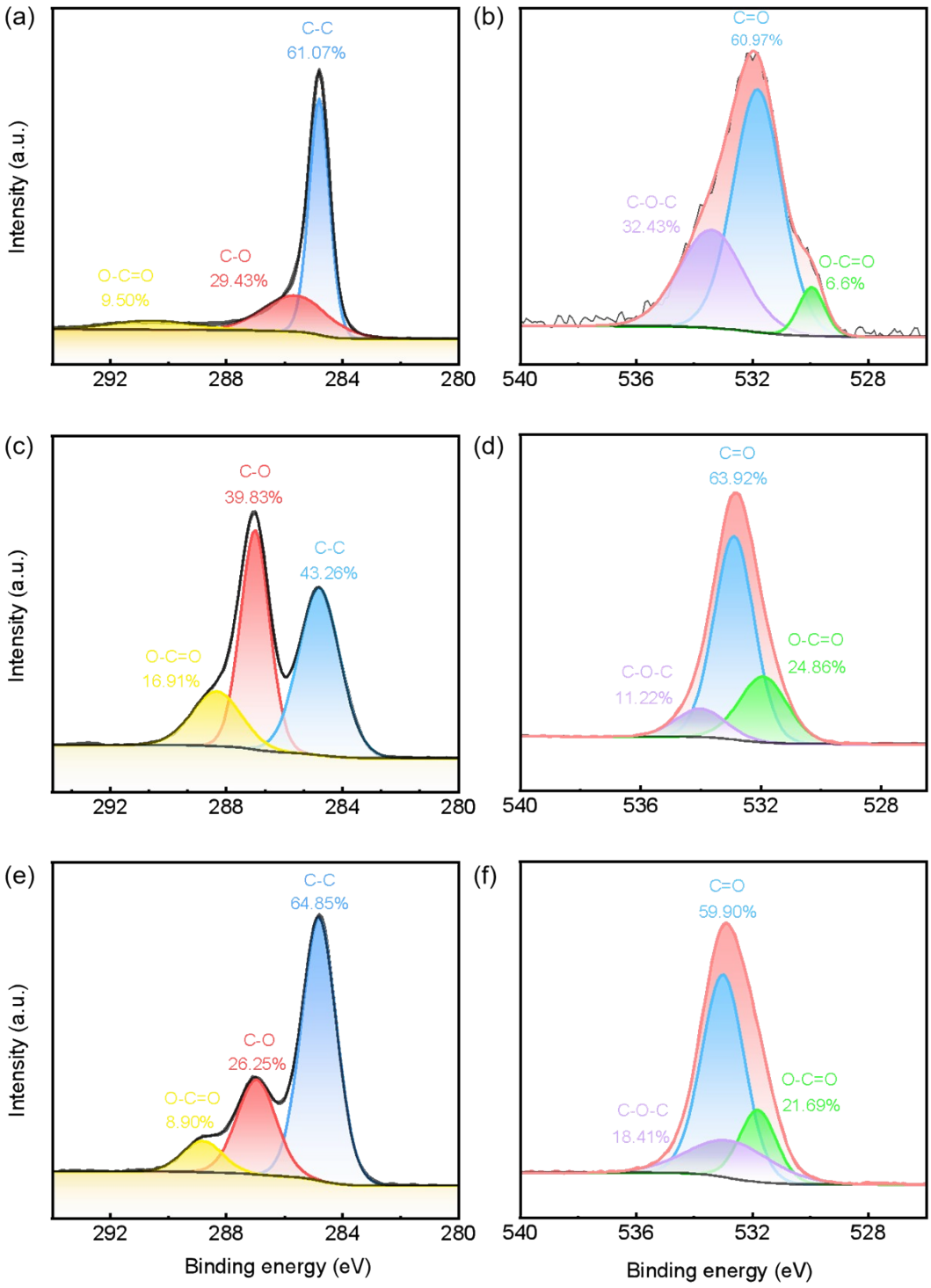

Figure S2. C 1s spectrum of (a) spent graphite, (c) graphite oxide, and (e) graphene oxide (GO) ; O 1s spectrum of (b) spent graphite, (d) graphite oxide, and (f) graphene oxide (GO).

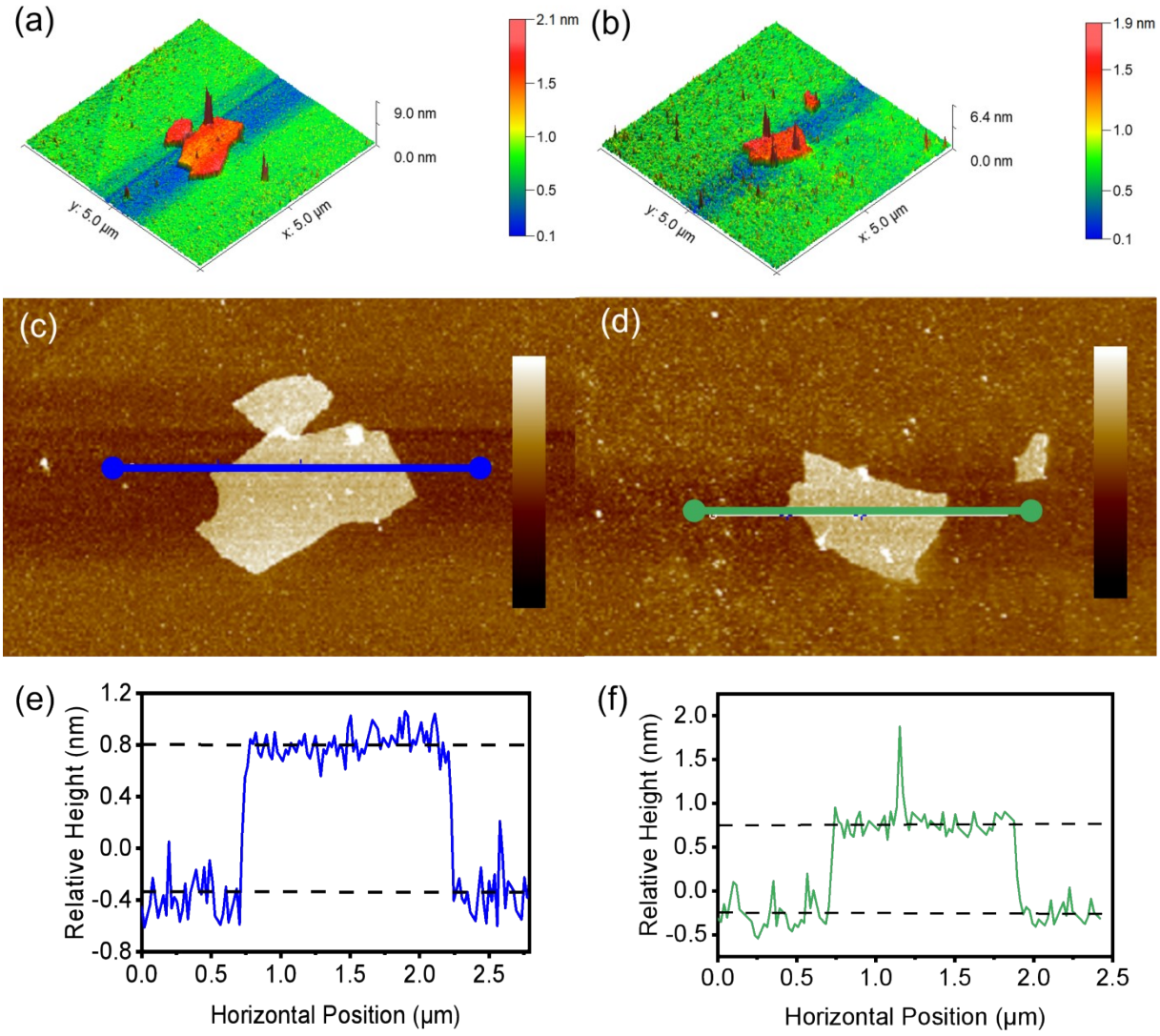

Figure S3. (a, b) AFM 3D image; (c, d) AFM surface image of graphene oxide (GO) nanosheet; (e, f) Size of graphene oxide (GO) nanosheet.

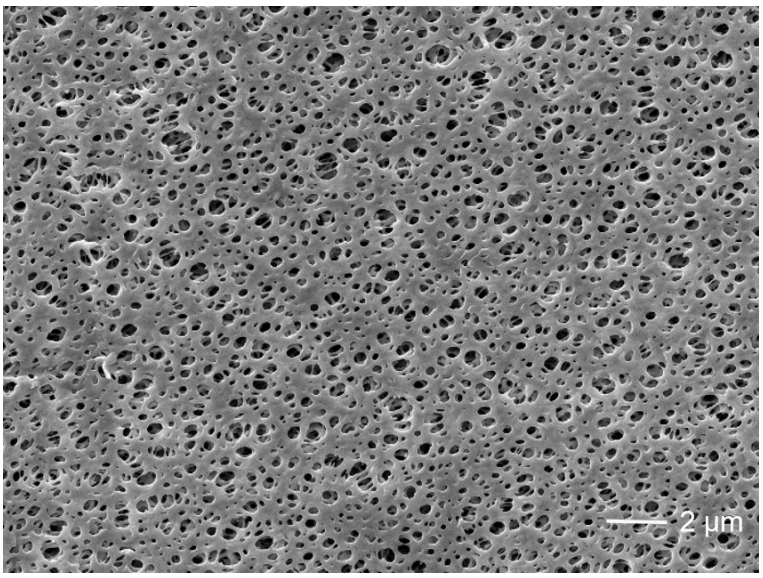

Figure S4. SEM images of the polyethersulfone (PES).

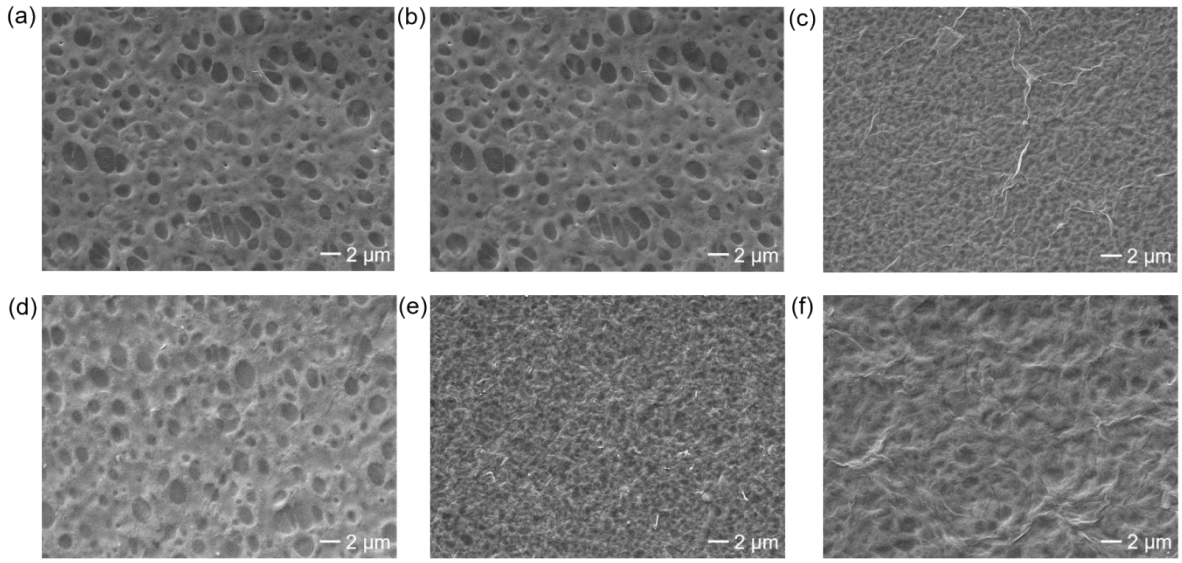

Figure S5. SEM images of the graphene oxide (GO) membrane (a, b, and c) and graphene oxide-polyethyleneimine (GO-PEI) membrane (d, e, and f) surface with the different graphene oxide (GO) deposition amounts: (a, d) 0.15g·m^{-2}; (b, e) 0.3 g·m^{-2}; (c, f) 0.6 g·m^{-2}.

(a)

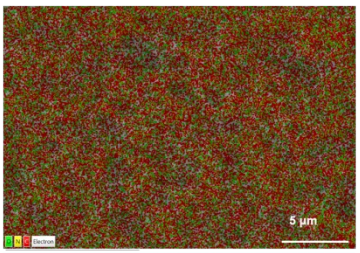

Element	Wt %	Atomic %
C	71.54	77.00
N	0.00	0.00
O	28.46	23.00

(b)

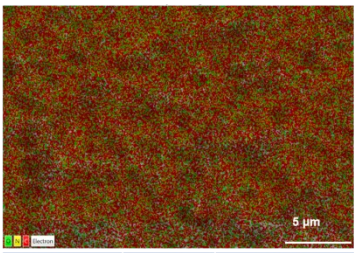

Element	Wt %	Atomic %
C	71.83	77.26
N	0.00	0.00
O	28.17	22.74

(c)

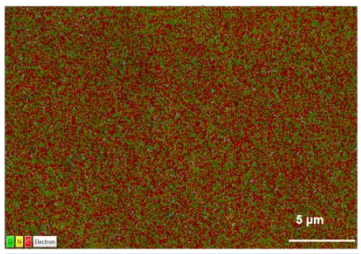

Element	Wt %	Atomic %
C	71.81	77.24
N	0.00	0.00
O	28.19	22.76

(d)

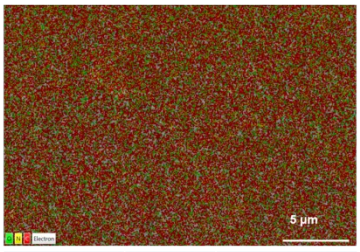

Element	Wt %	Atomic %
C	66.70	72.13
N	7.32	6.79
O	25.97	21.08

(e)

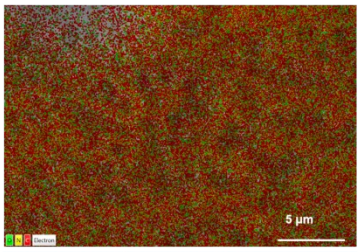

Element	Wt %	Atomic %
C	64.45	69.95
N	9.29	8.65
O	26.26	21.40

(f)

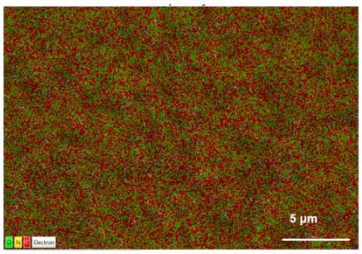

Element	Wt %	Atomic %
C	65.83	71.03
N	11.22	10.38
O	22.95	18.59

Figure S6. EDS of the graphene oxide (GO) membrane (a, b, and c) and graphene oxide-polyethyleneimine (GO-PEI) membrane (d, e, and f) surface with the different graphene oxide (GO) deposition amounts:: (a, d) 0.15g·m^{-2}; (b, e) 0.3 g·m^{-2}; (c, f) 0.6 g·m^{-2}.

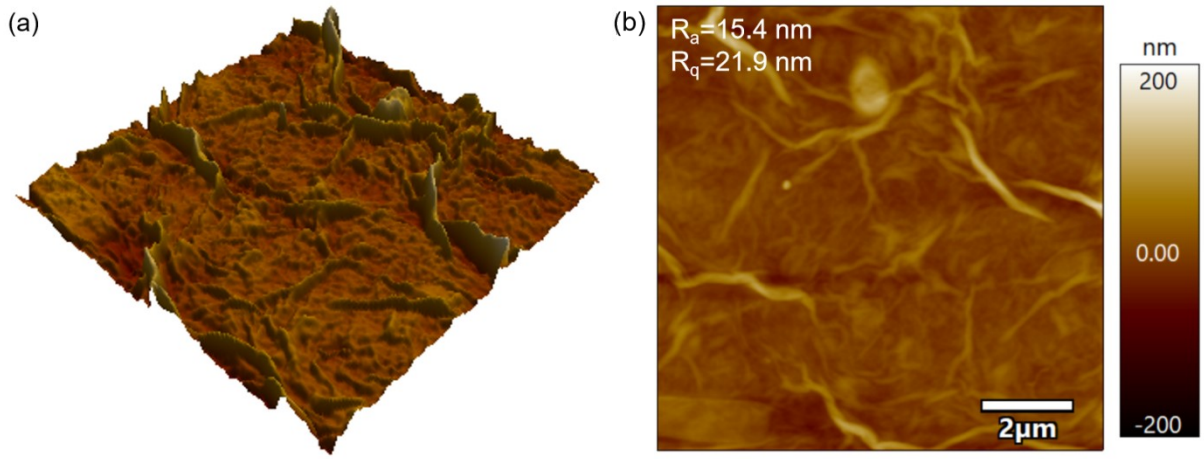

Figure S7. (a) AFM surface image, and (b) surface roughness of graphene oxide (GO) (0.6) membrane.

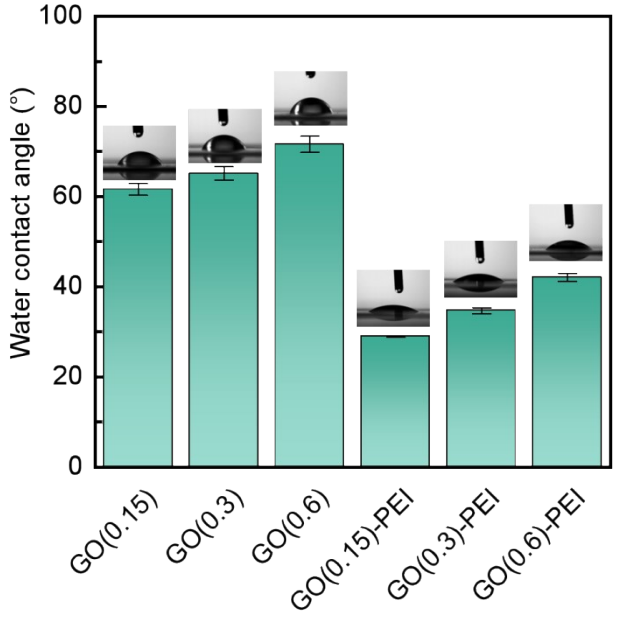

Figure S8. The contact angles for graphene oxide (GO) membranes and graphene oxide-polyethyleneimine (GO-PEI) membranes with the different loadings:0.15, 0.3, and 0.6 $g \cdot m^{-2}$.

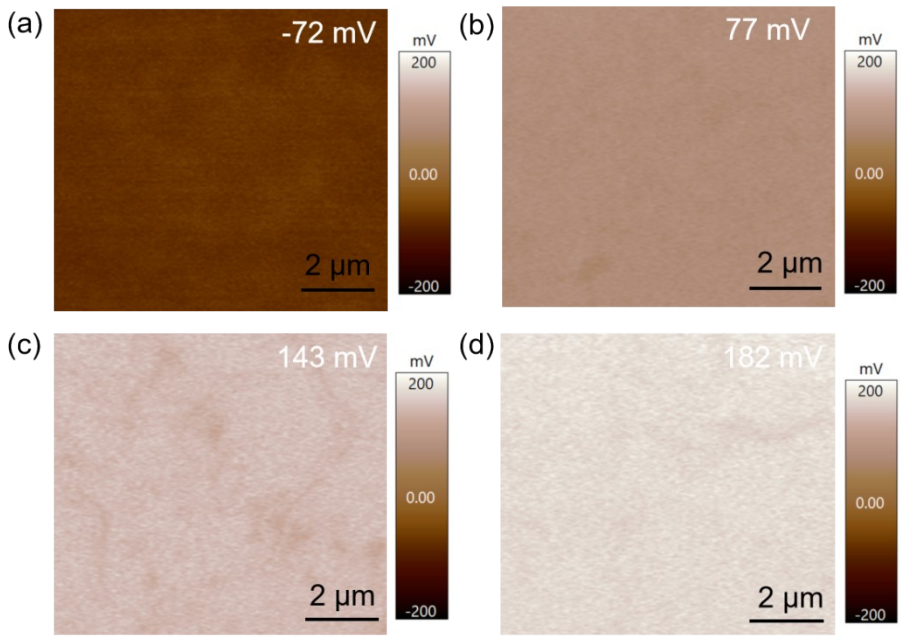

Figure S9. The potentials of (a) graphene oxide (GO) membrane, (b) GO (0.15)-polyethyleneimine (PEI) membrane, (c) GO (0.3)-PEI membrane, and (d) GO (0.6)-PEI membrane.

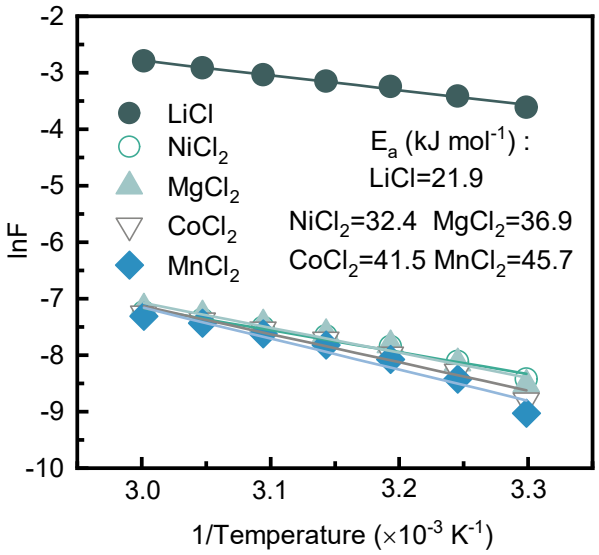

Figure S10. Activation energy for ion permeation through the GO(0.6)-PEI membrane.

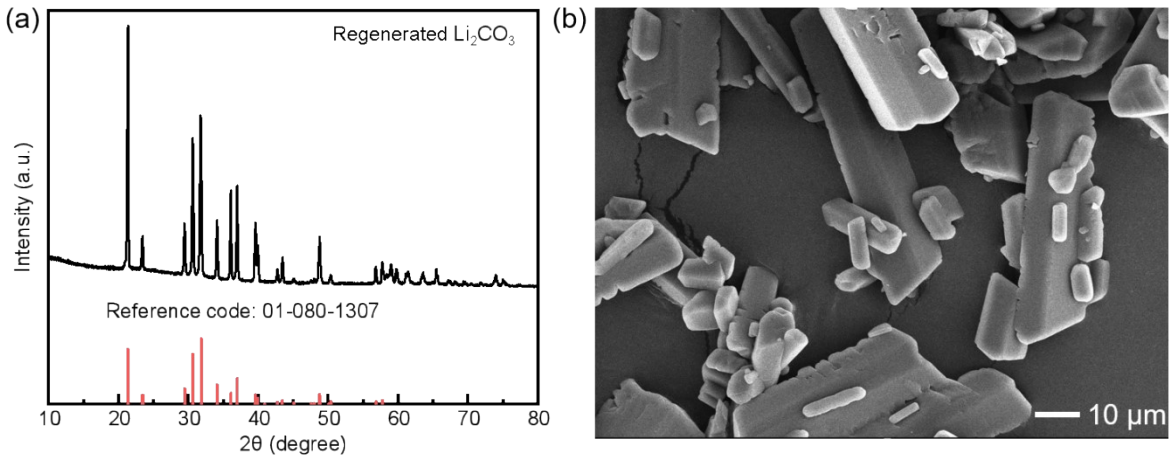

Figure S11. (a) XRD pattern, and (b) SEM image of the recovered Li_2CO_3 product.

References

(1) F., Sheng, B., Wu, X., Li, T., Xu, M., Shehzad, X., Wang, L., Ge, H., Wang and T., Xu. *Adv. Mater.*, 2021, **33**, 44, 2104404.

(2) S., Bing, W., Xian, S., Chen, Y., Song, L., Hou, X., Liu, S., Ma, Q., Sun and L., Zhang. *Matter*, 2021, **4**, 6, 2027-2038.

(3) H., Wu, H., Zhao, Y., Lin, X., Liu, L., Wang, H., Yao, Y., Tang, L., Yu, H., Wang and X., Wang. *J. Membrane Sci.*, 2023, **672**, 121468.

(4) Q., Wen, D., Yan, F., Liu, M., Wang, Y., Ling, P., Wang, P., Kluth, D., Schauries, C., Trautmann, P., Apel, W., Guo, G., Xiao, J., Liu, J., Xue and Y., Wang. *Adv. Funct. Mater.*, 2016, **26**, 32, 5796-5803.

(5) S., Liang, S., Wang, L., Chen and H., Fang. *Sep. Purif. Technol.*, 2020, **241**, 116738.

(6) Z., Zhou, D., Shinde, D., Guo, L., Cao, R., Nuaimi, Y., Zhang, L., Enakonda and Z., Lai. *Adv. Funct.*, 2021, **32**, 6, 2108672.

(7) T., Foller and R., Joshi. *ACS Nano.*, 2021, **15**, 6, 9201-9203.

(8) Y., Kang, T., Hu, Y., Wang, K., He, Z., Wang, Y., Hora, W., Zhao, R., Xu, Y., Chen, Z., Xie, H., Wang, Q., Gu and X., Zhang. *Nat. Commun.*, 2023, **14**, 4075.

(9) Z., Zhou, K., Zhao, H-Y., Chi, Y., Shen, S., Song, K-J., Hsu, M., Chevalier, W., Shi and K., Agrawal. *Nat. Commun.*, 2024, **15**, 4006.

(10) B., Niu, J., Xiao and Z., Xu. *J. Hazard. Mater.*, 2022, **439**, 129678.

(11) Q., Li, Y., Liu, Y., Jia, Y., Ji, F., Yan, J., Li, Y., Mohammad and B., He. *J. Membrane Sci.*, 2023, **677**, 121634.

(12) W., Li, C., Shi, A., Zhou, X., He, Y., Sun and J., Zhang. *Sep. Purif. Technol.*, 2017, **186**, 233-242.

(13) J., Lu, C., Dai, S., Li, D., Zou, Y., Sun and W., Jing. *Sep. Purif. Technol.*, 2024, **338**, 126508.

(14) F., Sheng, B., Wu, X., Li, T., Xu, M. A., Shehzad, X., Wang, L., Ge, H., Wang and T. Xu. *Adv. Mat.*, 2021, **33**, 2104404.

(15) R., Tan, A., Wang, R., Malpass-Evans, R., Williams, E. W., Zhao, T., Liu, C., Ye, X., Zhou, B. P., Darwich, Z., Fan, L., Turcani, E., Jackson, L., Chen, S. Y., Chong, T., Li, K. E., Jelfs, A. I., Cooper, N. P., Brandon, C. P., Grey, N. B., McKeown and Q., Song. *Nat. Mater.*, 2020, **19**, 195-202.